

Flaw Simulation in Castings

Domingo Mery

Department of Computer Engineering

University of Santiago, Chile

Av. Ecuador 3659, Santiago de Chile

dmery@ieee.org

<http://www.diinf.usach.cl/~dmery>

August 9, 2001

Abstract

In order to evaluate the sensitivity of defect inspection systems, it is convenient to examine simulated data. This gives the possibility to tune the parameters of the inspection method and to test the performance of the system in critical cases. Among the non-destructive testing and evaluation community there are three approaches that produce this simulated data. The first technique attempts to simulate flaws by superimposing masks with different grey values onto real x-ray images. The second approach makes a simulation of the entire x-ray imaging process, in which casting and flaws are simulated using CAD models. The third method simulates only the flaws (and not the whole x-ray image of the object under test) by superimposing projections of 3D models onto real x-ray images. In this paper, a review of the mentioned approaches of flaw simulation in castings is presented. References, advantages, disadvantages and examples are given for each technique.

Keywords: automated inspection, flaw simulation, CAD-models, aluminium castings, radiographic examination.

1 Introduction

Radioscopy is increasingly being used as a tool for non-destructive testing in industrial production. An example is the serial examination of cast light-alloy workpieces used in the car industry, like aluminium wheels and steering

gears [7]. The material defects occurring in the casting process such as cavities, gas, inclusions, and sponging must be detected to satisfy the safety requirements; consequently, it is necessary to check 100% of the parts. Since most defects are not visible, x-ray imaging is used for this task. An example of a radioscopic image is shown in Figure 1.

Over the past decades radioscopic systems have been introduced in the automotive manufacturing industry in order to detect flaws automatically without human interaction [1, 2, 6]. Over the years, they have not only increased quality through repeated objective inspections and improved processes, but have also increased productivity through decreased labour cost [10, 8].

An automated radioscopic system is schematically presented in Figure 2. The inspection is typically performed in the five following steps: *i)* the *manipulator* places the casting in the desired position; *ii)* the *x-ray tube* generates an x-ray image of the casting via central projection; *iii)* the x-ray image is detected by the fluorescent entrance screen of the *image intensifier*, amplified and depicted onto a phosphor screen. The image intensifier converts the x-ray image to a visible radioscopic image; *iv)* the guided and focussed image is registered by the *CCD-camera*; and *v)* the *image processor* converts the analogue video signal, transferred by the CCD-camera, into a digital data stream. Digital image processing is used to improve and evaluate the radioscopic image.

In order to evaluate the performance of a method that inspects castings, it is convenient to examine simulated data. This evaluation gives the possibility of tuning the parameters of the inspection method and of testing how the method works in critical cases. Among the non-destructive testing and

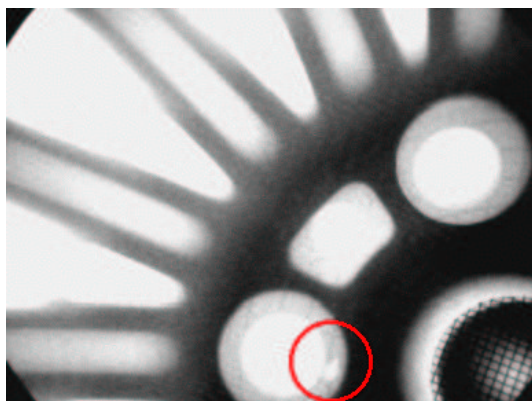


Figure 1: A real flaw in a radioscopic image of an aluminium wheel.

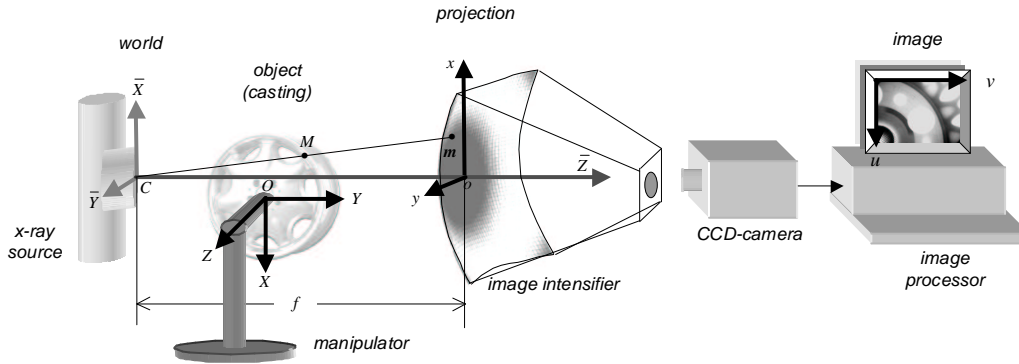


Figure 2: Diagram of a radiosopic imaging system.

evaluation community there are three approaches that produce this simulated data:

- *masks superimposition onto real x-ray images,*
- *CAD models for castings and flaws, and*
- *CAD model for flaws only and superimposition onto real x-ray images.*

The first technique attempts to simulate flaws by superimposing masks with different grey values onto real x-ray images. The second approach makes a simulation of the entire x-ray imaging process, in which casting and flaws are simulated using CAD models. The third method simulates only the flaws (and not the whole x-ray image of the object under test) by superimposing projections of 3D models onto real x-ray images according to the attenuation law for x-rays.

In this paper a description of these three techniques is presented as follows. The mask superimposition method is outlined in Section 2. A brief overview of the second technique that uses CAD models for castings and flaws is presented in Section 3. Section 4 describes the method that only simulates the flaws by superimposing 3D models of flaws onto real x-ray images. References, advantages, disadvantages, and examples for each technique are given. Finally, Section 5 presents concluding remarks and comparisons.

2 Masks superimposition

The first technique attempts to simulate flaws by superimposing masks with different grey values onto real x-ray images [6, 5, 2]. This approach is quite

simple, because it does not need any complex 3D model of the object under test nor of the flaw. Additionally, it offers a real x-ray image with real disturbances (with simulated flaws).

In this technique, the original grey value I_o of a pixel (u, v) of an x-ray image is altered by:

$$I_n(u, v) = M(u - u_0, v - v_0)I_o(u, v), \quad (1)$$

with $I_n(u, v)$ the new grey value and M the mask that is centred in pixel (u_0, v_0) , where $M(i, j)$ is defined in the interval $-\frac{N}{2} \leq i \leq \frac{N}{2}$ and $-\frac{M}{2} \leq j \leq \frac{M}{2}$. The masks shown in Figures 3a and 3b are normally used by this technique. They can mathematically defined by:

- **Square mask:**

$$M(i, j) = a \quad (2)$$

- **Circular mask:**

$$M(i, j) = \begin{cases} a & \text{if } \sqrt{i^2 + j^2} \leq r \\ 0 & \text{elsewhere} \end{cases} . \quad (3)$$

The flaws simulated by square and circle masks differ significantly from the real ones as shown in Figure 4. The reason being that a real flaw does not look like a projection of a square or disc. This method can only be used in restricted cases.

An improvement of these masks can be obtained using the third mask illustrated in Figure 3c that corresponds to a visualisation technique called *splatting* [12]. In this technique the projection of a 3D flaw can be simulated, in which the projected flaw is assumed as a 2D Gaussian. The scale, position,

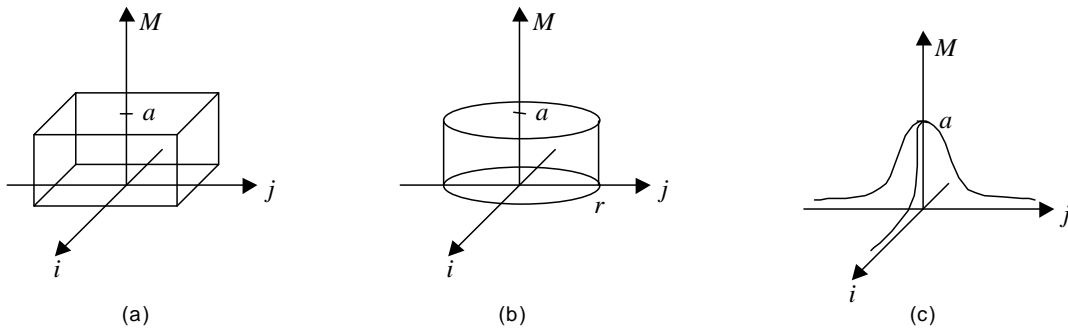


Figure 3: (a) Square mask. (b) Circle mask. (c) Gaussian mask.

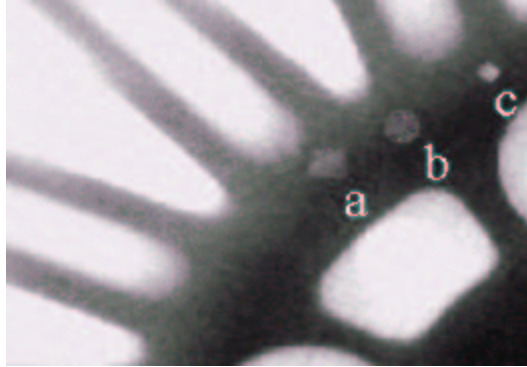


Figure 4: Flaw simulation using (a) square, (b) circle, and (c) Gaussian masks.

and orientation of the Gaussian are adjusted in order to obtain the desired projected flaw. Mathematically the Gaussian mask is given by:

$$M(i, j) = a \exp\left(-\frac{i^2}{2\sigma_i^2}\right) \exp\left(-\frac{j^2}{2\sigma_j^2}\right) \quad (4)$$

An example is shown in Figure 4. Although this technique offers a better flaw simulation in comparison with the other two masks, its simulation corresponds to the projection of a 3D flaw, that differs considerably from real flaws. Real flaws like bubbles or round blowholes are clearly delimited in the casting material, and its projection does not offer a smooth profile as presented in a Gaussian function [9].

3 CAD models for casting and flaw

The second approach makes a simulation of the entire x-ray imaging process [11, 3]. In this approach, the characteristic of the x-ray source, the geometry, and material properties of objects and their defects, as well as the imaging process itself are modelled and simulated independently. Complex objects and defect shapes can be simulated using CAD models.

The principle of the simulation is shown in Figure 5. The x-ray may intersect different parts of the object. For each pixel (u, v) of the simulated image the intersection points between the modelled object with the corresponding x-ray beam that is projected into the pixel (u, v) are calculated.

X-ray attenuation law is the basis of this simulation approach [4]:

$$\varphi(x) = \varphi_0 e^{-\mu x}, \quad (5)$$

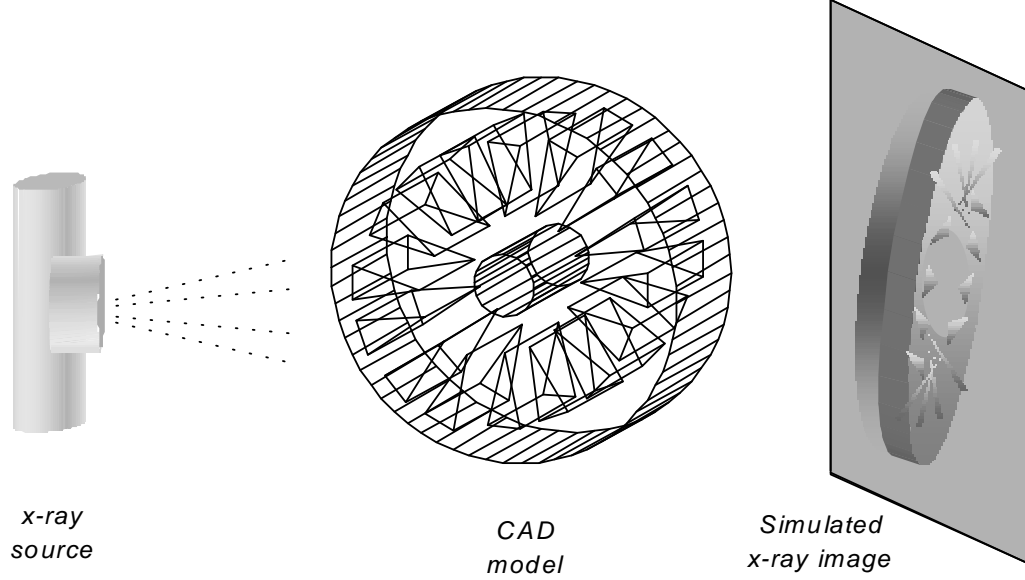


Figure 5: X-ray image simulation using CAD models.

where φ_0 is the incident radiation intensity, φ the transmitted intensity, x the thickness of the object under test and μ is the energy dependent linear attenuation coefficient associated with the material. According to the attenuation law, the grey value of a pixel of the simulated image can be computed as:

$$I = A\varphi_0(E)\Delta\Omega \exp\left(-\sum_i \mu_i(E)x_i\right) + B \quad (6)$$

where A and B are linear parameters of I , $\varphi_0(E)$ is the incident radiation intensity with energy E , $\Delta\Omega$ is the solid angle that corresponds to the pixel observed from the source point, $\mu_i(E)$ designates the attenuation coefficient associated with the material i at the energy E , and x_i the total path length through the material i . Since the x-ray source is modelled as a raster of point sources, rays from every source point are traced to all pixels of the simulated image.

A flaw like a cavity can be simulated when a material with no absorption is considered. In Figure 6 this simulation is shown schematically. An x-ray beam penetrates an object which has a cavity with thickness d . In this case, from (5) the transmitted radiation φ_d is given by:

$$\varphi_d = \varphi(x - d) = \varphi_0 e^{-\mu(x-d)} = \varphi(x) e^{\mu d}, \quad (7)$$

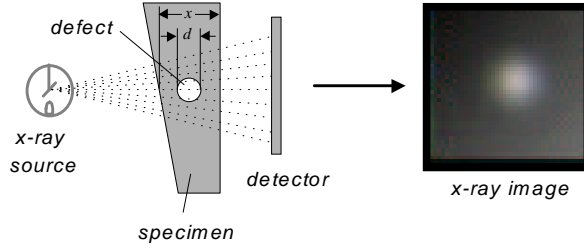


Figure 6: Differential absorption in a specimen.

where we assume that the absorption coefficient of the cavity is zero. If the flaw is an incrustated material, its absorption coefficient μ_d must be considered in (7):

$$\varphi_d = \varphi_0 e^{-\mu(x-d)} e^{-\mu_d d} = \varphi(x) e^{d(\mu - \mu_d)}. \quad (8)$$

In [11], complicated shapes for 3D flaws are reported. The defect model is coupled with a CAD interface yielding 3D triangulated objects. Using this technique simulation of other kind of flaws like cracks can be obtained.

Although this approach offers excellent flexibility in setting the objects and flaws to be tested, it presents the following three disadvantages to the evaluation of the inspection methods' performance: *i*) the x-ray image of the object under test is simulated (it would be better if we could count on real images with simulated flaws); *ii*) the simulation approach is only available when using a sophisticated computer package; *iii*) the computing time is expensive.

4 CAD models for flaws only

This approach simulates only the flaws and not the whole x-ray image of the object under test [9]. This method can be viewed as an improvement of the first mentioned technique (Section 2) and the 3D modelling for the flaws of the second one (Section 3). In this approach, a 3D modelled flaw is projected and superimposed onto real x-ray images of a homogeneous object according to the exponential attenuation law for x-rays (5).

The grey value I registered by the CCD-camera can be expressed as a linear function of the transmitted radiation φ :

$$I(x) = A\varphi(x) + B, \quad (9)$$

where A and B are the linear parameters of I , and x the thickness of the object under test. If the penetrated object has a cavity with thickness d as

shown in Figure 6 the transmitted radiation is given by (7). In this case the grey value registered by the CCD camera is calculated then from (9) as:

$$I(x - d) = A\varphi(x)e^{\mu d} + B. \quad (10)$$

Substituting the value of $A\varphi(x)$ from (9) we see that (10) may be written as:

$$I(x - d) = (I(x) - B)e^{\mu d} + B. \quad (11)$$

Parameter B can be estimated as follows: the maximal grey value I_{max} in an x-ray image is obtained when the thickness is zero. Additionally, the minimal grey value I_{min} is obtained when the thickness is x_{max} . Substituting these values in (9), it yields:

$$\begin{cases} I_{max} &= A\varphi_0 + B \\ I_{min} &= A\varphi_0 e^{-\mu x_{max}} + B \end{cases} .$$

From these equations, one may compute the value for B :

$$B = I_{max} - \Delta I / (1 - e^{-\mu x_{max}}) , \quad (12)$$

where $\Delta I = I_{max} - I_{min}$. Usually, I_{max} and I_{min} are 255 and 0 respectively.

Using equation (11), we can alter the original grey value of the x-ray image $I(x)$ to simulate a new image $I(x - d)$ with a flaw. A 3D flaw can be modelled, projected, and superimposed onto a real x-ray image. The new grey value of a pixel, where the 3D flaw is projected, depends only on four parameters: a) the original grey value $I(x)$; b) the linear absorption coefficient of the examined material μ ; c) the maximal thickness observable in the x-ray image x_{max} ; and d) the length of the intersection of the 3D flaw with the modelled x-ray beam d , that is projected into the pixel.

In [9] an ellipsoidal model for a flaw is described in detail. Using this tool a simulation of an ellipsoidal flaw of any size and orientation can be done in any position of the casting. This model can be used for flaws like blowholes and other round defects. Two examples are shown in Figure 7. Due to the irregularity of the grey values of the simulated flaw, it seems to be real. Other Complex defect shapes can be simulated using CAD models.

This technique presents two advantages: in comparison with the first technique the simulation is better; in comparison with the second one we gain more speedup from the reduced computational complexity. However, the model used in this method has four simplifications that were not done by the second simulation technique: *i)* the x-ray source is assumed as a source point; *ii)* there is no consideration about the noise in the model; *iii)* there is no consideration about the solid angle $\Delta\Omega$ of the x-ray beam that is projected onto a pixel; and *iv)* the spectrum of the radiation source is monochromatic.

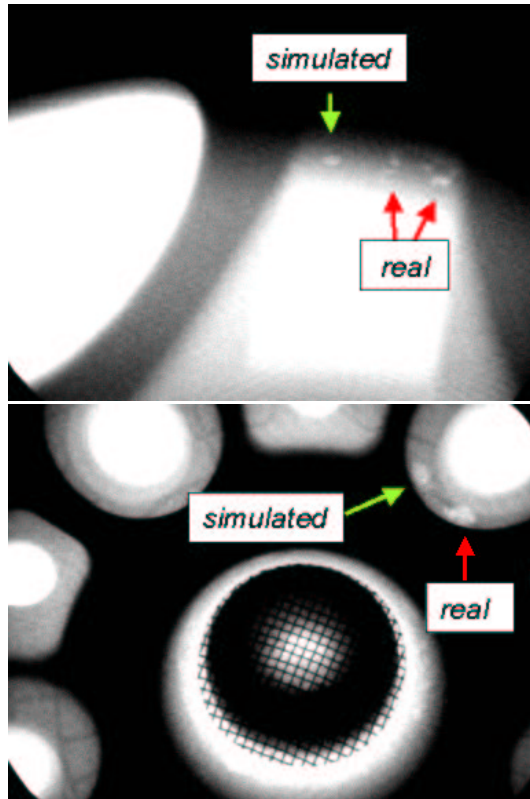


Figure 7: Simulated ellipsoidal flaws using third technique.

5 Summary

Three techniques for the simulation of defects in x-ray images of castings has been presented. The first technique attempts to simulate flaws by superimposing masks with different grey values onto real x-ray images. The second approach makes a simulation of the entire x-ray imaging process, in which casting and flaws are simulated using CAD models. The third method simulates only the flaws (and not the whole x-ray image of the object under test) by superimposing projections of 3D models onto real x-ray images according to the attenuation law for x-rays. Table 1 summarises the advantages and disadvantages of the methods.

Mask superimposition is the simplest technique. However, it can only be used in restricted cases. The reason being that real flaws do not look like rough projections of squares, discs or Gaussian functions.

By modelling casting and flaws in 3D we obtain very good simulations, because this technique offers excellent flexibility in setting the objects and

Method	Flaw 3D Geometry	Casting 3D Geometry	Complex Flaws	Computational time	Flaw Simulation	Object x-ray image
Masks Superimposition	no required	no required	no	very fast	very bad	real
CAD Models for Casting & Flaws	required	required	yes	very slow	very good	simulated
CAD Models for Flaws	required	no required	yes	fast	good	real

Table 1: Advantages and disadvantages of the simulation techniques.

flaws to be tested. However, it would be better if we could count on real images with simulated flaws. Additionally, this technique is only available when using a sophisticated computer package, and the computing time is very expensive.

The third technique, in which only the flaws are simulated, presents two advantages in comparison with the other ones. The results are better than those obtained with the first one; and the simulation is considerably faster than the simulation of the second one. However, the model used by this method presents some simplifications that were not done by the second technique. For this reason, the accuracy in the flaw simulation of the second method seems to be better than the third technique.

If we want to evaluate the sensitivity of defect inspection systems, it would be better if we could examine real x-ray images with simulated flaws. In this sense the third technique has a very good performance. However, in the future the model used by this technique must be consider the assumptions of the second one.

Acknowledgments

The author is grateful to Prof. Dr.-Ing. D. Filbert of the Technical University of Berlin for his contribution to this research. The radioscopic material of this paper was obtained with the help of Dr. J.-M. Kosanetzky and Dr.-Ing. K. Bavendiek of YXLON International X-Ray GmbH (Hamburg).

References

- [1] H. Boerner and H. Strecker. Automated x-ray inspection of aluminum casting. *IEEE Trans. Pattern Analysis and Machine Intelligence*, 10(1):79–91, 1988.

- [2] D. Filbert, R. Klatte, W. Heinrich, and M. Purschke. Computer aided inspection of castings. In *IEEE-IAS Annual Meeting*, pages 1087–1095, Atlanta, USA, 1987.
- [3] N. Freud, P. Duvauchelle, and D. Babot. Simulation of x-ray NDT imaging techniques. In *Proceedings of the 15th World Conference on Non-Destructive Testing (15th-WCNDT)*, Rome, Oct. 15-21 2000.
- [4] H. Haken and H.C. Wolf. *The Physics of Atoms and Quanta: Introduction to Experiments and Theory*. Springer, Berlin, Heidelberg, 5 edition, 1996.
- [5] H. Hecker. *A new Method to Process X-Ray Images in the Automated Inspection of Castings*. PhD thesis, Institute for Measurement and Automation, Faculty of Electrical Engineering, Technical University of Berlin, 1995. (in German).
- [6] W. Heinrich. *Automated Inspection of Castings using X-Ray Testing*. PhD thesis, Institute for Measurement and Automation, Faculty of Electrical Engineering, Technical University of Berlin, 1988. (in German).
- [7] J.-M. Kosanetzky and H. Putzbach. Modern x-ray inspection in the automotive industry. In *Proc. 14th World Conference of NDT (14th-WCNDT)*, New Delhi, Dec. 8-13 1996.
- [8] D. Mery. *Automated Flaw Detection in Castings from Digital Radioscopic Image Sequences*. Verlag Dr. Köster, Berlin, 2001. (Ph.D. Thesis in German).
- [9] D. Mery. A new algorithm for flaw simulation in castings by superimposing projections of 3D models onto x-ray images. In *Proceedings of the XXI International Conference of the Chilean Computer Science Society SCCC-2001*, Punta Arenas, 6-8 Nov. 2001. IEEE Computer Society Press. In Press.
- [10] D. Mery, Th. Jaeger, and D. Filbert. Automated quality control of castings – state of the art. *tm - Technisches Messen*, 68(7-8), 2001. (in German).
- [11] G.-R. Tillack, C. Nockemann, and C. Bellon. X-ray modelling for industrial applications. *NDT & E International*, 33(1):481–488, 2000.
- [12] L. Westover. Footprint evaluation for volume rendering. *Proceedings of SIGGRAPH*, 24(4):367–376, 1990.

Domingo Mery received the Diploma (M.Sc.) degree in Electrical Engineering from the Technical University of Karlsruhe, Germany, in 1992, and the Ph.D. degree with honours at the Technical University of Berlin, in 2000. During 1993 – 1996, he was a Research Assistant at the Department of Electrical Engineering at the Catholic University of Chile. From 1996 to 2000, he was a Research Scientist at the Institute for Measurement and Automation Technology at the Technical University of Berlin with the collaboration of Philips and YXLON X-Ray International. From 1989 to 1992 he was a recipient of a Scholarship from the Konrad-Adenauer-University, and from 1996 to 2000 of a Scholarship from the German Academic Exchange Service (DAAD) for his Ph.D. work. Since 2001 he is Assistant Professor at the Department of Computer Engineering at the University of Santiago, Chile . His research interests include image processing for automated inspection, x-ray imaging, real-time programming and computer vision.